POLİTEKNİK DERGİSİ

JOURNAL of POLYTECHNIC

ISSN: 1302-0900 (PRINT), ISSN: 2147-9429 (ONLINE)
URL: http://dergipark.org.tr/politeknik

Improvement of dynamic wheel load oscillations by coupling pitch motion into bounce motion during pitching motion of passenger vehicle

Binek taşıtın başvurma hareketi sırasında başvurma hareketinin kalkım hareketine kuplajı ile dinamik tekerlek yük salınımlarının iyileştirilmesi

Yazar(lar)(Author(s)): *Hakan KÖYLÜ*

ORCID: 0000-0002-3548-0484

Bu makaleye şu şekilde atıfta bulunabilirsiniz (To cite to this article): Koylu H., "Improvement of dynamic wheel load oscillations by coupling pitch motion into bounce motion during pitching motion of passenger vehicle", ***Politeknik Dergisi***, 24(4):1473-1489,(2021).

Erişim linki (To link to this article): http://dergipark.org.tr/politeknik/archive

DOI: **10.2339/politeknik.641156**

Improvement of Dynamic Wheel Load Oscillations by Coupling Pitch Motion into Bounce Motion during Pitching Motion of Passenger Vehicle

Highlights

- *Reductions in both the front and rear dynamic wheel load oscillations with oscillation center position change*
- *The reductions depend on how the damping level of the shock absorber on a wheel will vary with respect to the change in the suspension spring*
- *The ride comfort is not deteriorated as well as road holding*

Graphical Abstract

In this study, the locations of pitch and bounce ossilation centers that could reduce the front and rear dynamic load oscillations occurring between the tire and the rim during the pitch motion were determined.

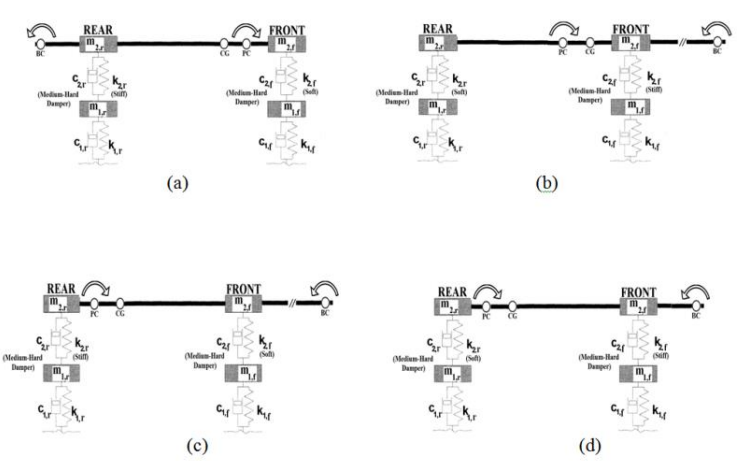

Figure A. The variations for changing of pitch and bounce centers

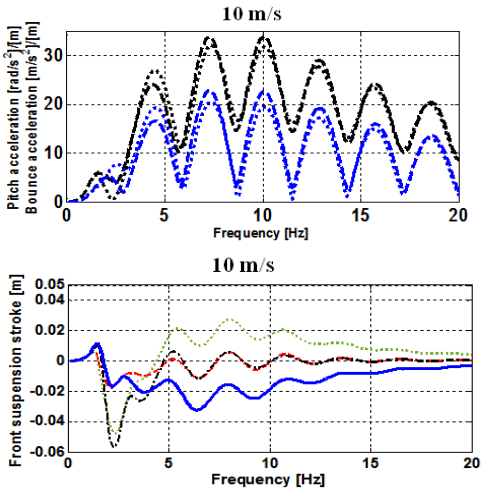

Figure B. The ride comfort and stroke analysis

Aim

The purpose of this paper is to determine the location of pitch and bounce oscillation centers which reduce dynamic wheel loads.

Design & Methodology

The half car model, which two quarter car models are combined by changing suspension stiffness and damping ratio and coupling the pitch motion to bounce motion, was used to change the location of oscillation centres, In this way, the effects of changes in front suspension settings were reflected on those of rear suspension through different stiffnesses and damping ratios.

Originality

Dynamic wheel load oscillations have been improved without worsening comfort with only passive suspension elements not active suspension elements..

Findings

If the oscillation center is changed depending on suspension stiffness without changing front and rear damping capacities, both of front and rear wheel load oscillations are not improved. However, if the pitch and bounce centers are on same front wheel, both of front and rear oscillations can be reduced.

Conclusion

The most convenient oscillation center location to reduce dynamic wheel load oscillations has been determined without deteriorating ride comfort. This improvement has been obtained by varying available coupling with the changes in location of oscillation center.

Declaration of Ethical Standards

The author(s) of this article declare that the materials and methods used in this study do not require ethical committee permission and/or legal-special permission.

Improvement of Dynamic Wheel Load Oscillations by Coupling Pitch Motion into Bounce Motion during Pitching Motion of Passenger Vehicle

Araştırma Makalesi / Research Article

Hakan KÖYLÜ*

Department of Automotive Engineering, Faculty of Technology, Kocaeli University, Kocaeli, Turkey.

(Geliş/Received : 01.11.2019 ; Kabul/Accepted : 02.07.2020 ; Erken Görünüm/Early View : 13.07.2020)

ABSTRACT

The aim of this study is to determine the oscillation center position change that can reduce the dynamic wheel load oscillations during the pitching motion. For this purpose, the pitch and heave motions were coupled to each other during the pitch motion by changing the positions of the pitch and heave oscillation centers according to each other. The degree of coupling is determined by the front and rear spring stiffness. For this, the half-vehicle model that can be coupled to the two-quarter vehicle model with the suspension components were used. With this model, the effects of coupling on dynamic wheel load oscillations were examined in frequency domain according to the location of the center of gravity and vehicle speed. The results showed that the position changes of the oscillation centers can reduce both the front and rear dynamic wheel load oscillations, and this will be slightly affected by vehicle speed variation. It has also been found that this improvement depends on how the damping level of the shock absorber on a wheel will vary with respect to the change in the suspension spring.

Keywords: Suspension system, coupling effect, oscillation center, pitch and bounce motion, dynamic wheel load.

Binek Taşıtın Başvurma Hareketi Sırasında Başvurma Hareketinin Kalkım Hareketine Kuplajı İle Dinamik Tekerlek Yük Salınımlarının İyileştirilmesi

ÖZ

Bu çalışmanın amacı, başvurma hareketi sırasında dinamik tekerlek yükü salınımlarına azaltabilecek salınım merkezi konum değişiminin tespit edilmesidir. Bunun için başvurma ve kalkım salınım merkezlerinin konumları birbirine göre değiştirilerek başvurma hareketi sırasında kalkım ve başvurma hareketi birbirine kuplaj edilmiştir. Kuplajın derecesi ön ve arka yay sertlikleri ile belirlenmiştir. Bunun için süspansiyon elemanları ile iki çeyrek taşıt modelini kuplaj yapılabilecek yarım taşıt modeli kullanılmıştır. Bu model ile kuplajın dinamik tekerlek yük salınımlarına etkileri frekans boyutunda ağırlık merkezinin konumuna ve taşıt hızına göre incelenmiştir. Elde edilen sonuçlar, salınım merkezlerinin konum değişimlerinin hem ön hem de arka dinamik tekerlek yük salınımlarını azaltabileceğini ve bunun taşıt hızı değişiminden çok az etkileneceğini göstermiştir. Aynı zamanda, bu düzelmenin, bir tekerlek üzerindeki amortisörün sönümleme seviyesinin süspansiyon yayındaki değişime göre nasıl değişeceğine bağlı olduğu görülmüştür.

Anahtar Kelimeler: Süspansiyon sistemi, kuplaj, salınım merkezi, başvurma ve kalkım, dinamik tekerlek yükü.

1. INTRODUCTION

In vehicles, suspension systems play a great role in the enhancement of tyre-road contact. Under some driving and road conditions such as braking and acceleration, the contact may deteriorate. One of the most important and annoying conditions which degrade the contact is the pitch and bounce motions of vehicle body. Because, the road irregularities have constantly excited the suspension spring and damper elements during these motions. For this reason, the dynamic wheel load acting between wheel rim and road contact surface tyre becomes more severe [1, 2, 3]. Thus, the dynamic wheel load oscillations should be minimized to keep tire forces at desired level. Thus, either the passive suspension elements such as spring and damper or the active elements are used. In this study, the first case has been considered. Because, at present time, most modern road vehicles contain only passive suspension elements. This is due to the drawbacks associated with active technologies, such as increased cost, uncertain reliability, power consumption requirements, and inherent complexity. Therefore, alternative passive suspensions that provide better braking performance, pitch comfort and road contact are of great value in the automotive industry [4]. The most important of these suspensions is a coupled front and rear suspension which is the system in which a displacement at one wheel station can produce appropriate vertical displacements on other wheel stations. In coupled suspensions, front wheel is coupled to rear wheel by hardening or softening the passive spring or dampers as follows [5].

*Sorumlu Yazar (Corresponding Author)
e-posta : hkoylu@kocaeli.edu.tr

$$(2l_f C_f - 2l_r C_r)\frac{d}{dt} = 2l_f k_f - 2l_r k_r \quad (1)$$

Where c_f, c_r, k_f, k_r, l_f and l_r are front and rear damping coefficient and spring stiffness, distance of front and rear axles to center of gravity, respectively. While the spring is hardened or softened, the choosing of correct ratio of front–rear spring stiffness significantly affects the pitch response [6]. Therefore, pitching vibrations can be supressed with little degradation of bounce response by making the rear suspension stiffer than that of front suspension, since ratio of angular frequency of pitch (ω_p) to angular frequency of bounce (ω_b) is reduced [7, 8]. This is described as follows:

$$\frac{\omega_p}{\omega_b} = \sqrt{\frac{K_p m_s}{I_p K_b}} \quad (2)$$

where Ip, Kp and Kb and are pitch inertial moment, pitch and bounce stiffness, respectively. Therefore, the ratio can be decreased to improve the pitch vibrations by increasing the bounce stiffnes. For these reasons, the coupling between front and rear suspensions should be provided to reduce pitch amplitudes. Thus, the better dynamic wheel load oscillations and pitch comfort can be provided [9]. For this, the criteria and methods were designed to couple pitch motion to bounce motion. The following conditions have been proposed by [10, 11, 12] to couple the motions.

a) $k_{2,f}\, l_f > k_{2,r}$ **b)** $l_r\, k_{2,f}\, l_f < k_{2,r}\, l_r$ **c)** $k_{2,f}\, l_f = k_{2,r}\, l_r$ (3)

These conditions couple the pitch to bounce motion. In addition, the following condition is considered to couple damper forces [13,14].

$$c_{2,f}\, l_f = c_{2,r}\, l_r \quad (4)$$

Nagai et.al. have reported that the peaks of rear suspension decrease relative to those of front as the damping coefficient of coupled system increases [15]. Also, Dixon states that the damping of the pitch mode is largely dependent on the rear dampers [16]. In these studies related to the coupling, the optimum tuning of suspensions is also dependent on the vehicle speed for pitch minimization. Sharp et.al. has found that Olley's tuning gives an improved pitch displacement response above 10 m/s, but degrades it below 10 m/s [17]. The effects of vehicle speed on the dynamic wheel load and pitch comfort can be achieved through the wheelbase filtering effect [17,18], because the wheelbase filtering introduces a dependence of the vehicle system response to the vehicle speed [11]. It also refers to the effects of the time delay between the front and rear wheels on vehicle dynamics. Hence, the wheelbase filtering effects can reduce pitch response for each speed by providing different optimal suspension tuning [19].

As for the ride comfort, the trade off between ride safety and ride comfort is considered not to degrade the ride comfort while improving the ride safety, [5]. Recently, the research efforts have been focused on control systems of interconnected suspension system to overcome the compromise problems between the ride and the handling performance encountered in conventional suspensions. For this, the control algorithms were developed by using the coupling and decoupling methods. In some control applications, the pitch motion was hydraulically tuned to bounce motion to reduce pitch angle, pitch acceleration and dynamic tire force. In here, the coupling and decoupling methods are used for front and rear dampers to interconnect the corners of front and rear suspensions as shown in Eqs(1,3 and 4) [20]. In another control study, the pitching stifness and the ratio of pitch frequency to bounce frequency were considered to connect the front suspension to rear suspension. Also, Olley's rules were used in the control algorithms. His rules propose that the pitch and bounce frequencies must be close, and the bounce frequency should be less than 1.2 times the pitch frequency [5, 11, 12]. In addition, some criteria were considered to design the control rules for minimizing pitch acceleration. One of these criteria is related to the pitch frequency suggested by [11]. He explored that if the pitch natural frequency is too high with respect to that of bounce motion, the ride comfort can be affected. The other criterion is associated with pitch stiffness proposed by [21, 22]. They explored that the pitch-coupled suspension reduced dynamic wheel load and body acceleration responses of a passenger car by keeping the pitch stiffness at low level. As a result, many studies were conducted on the improving of pitch ride comfort by using methods coupling pitch to bounce motion. However, it was seen that it is not known whether the criteria and methods are appropriate to implement to the dynamic wheel loads during pitch motions. Also, the method to reduce dynamic wheel load provides to design interconnedted air suspension. For this, the changes in inside pressure of front and rear air springs enable to reduce dynamic wheel load oscillations on front and rear axles by varying inside presure of front and rear air springs according to variations of location of bounce and pitch center. For these reasons, in this study, the dyamic wheel load is investigated by using coupling effect through tuning of passive suspension stifness and the damping. For this, the half car model enabling to couple the pitch motion to bounce motion is designed by changing the oscillation centres. The conditions given in Eqs(3 and 4) are considered to change the oscillation center. In addition, the results are compared according to the forward speed of vehicle and the CG of vehicle body to determine the effects of wheelbase filtering on dynamic wheel laod oscillations. Also, the changes in natural frequencies of pitch and bounce motion as well as pitch stiffness are observed for the compromise between ride comfort and ride safety.

2. HALF CAR MODELING

2.1 Model Description

A half car model is modelled with four degrees of freedom to investigate the effects of pitch and bounce motions on dynamic wheel load oscillations with different locations of pitch and bounce oscillation centers as shown in Fig.1.

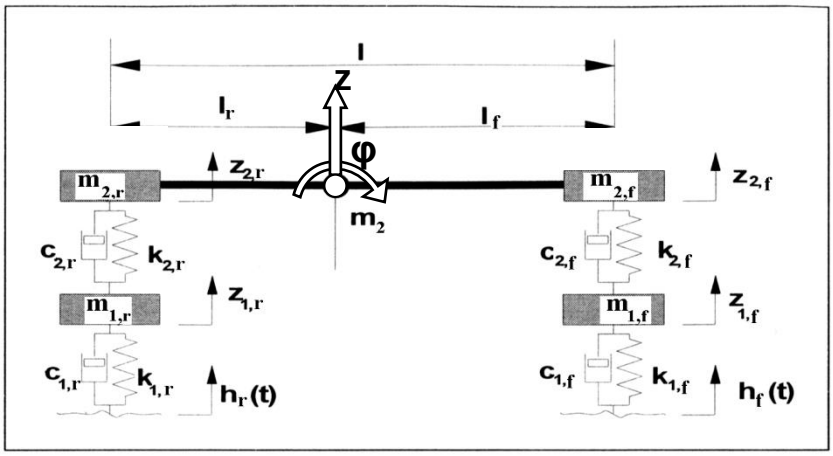

Figure 1. The half car model

This model is different from other conventional half car models. Because, in this model, the pitch and bounce motions are obtained with the front and rear vertical displacements of sprung mass as shown in Eqs. (5), (6) and (7). In this way, the vertical displacements are determined by vibration elements of suspension system and thus, the front and rear displacements are intervened by changing suspension stiffness and damping coefficient of damper. Also, the changes in vibration elements enable the location of pitch and bounce oscillation centers to change. Furthermore, the changes in location of pitch and bounce provide to couple the pitch motion to bounce motion through suspension stiffnesses and damping coefficients.

For this reason, the vertical displacements of the sprung and unsprung masses connected to front and rear axle are considered as generalized coordinates. Therefore, the coupling effect of pitch and bounce motion on dynamic wheel load oscillations is changed by different oscilation centers through vibration characteristics of suspension elements. In other words, the location of oscillation centers is changed through the coupling of different front and rear suspension elements. The basic vehicle parameters related to this car model and the variables calculated from the basic vehicle parameters are shown in Table 1.

Table 1. The parameters of the half car model

Parameters	Description
$m_{2,f}$	Front sprung mass
$m_{2,r}$	Rear sprung mass
$m_2 = m_{2,f} + m_{2,r}$	Vehicle body mass
$m_{1,f}$	Front unsprung mass
$m_{1,r}$	Rear unsprung mass
$f_{n,f}$	Natural frequency of front sprung mass
$f_{n,r}$	Natural frequency of rear sprung mass
$\omega_{n,f}=2\pi f_{n,f}$	Angular natural frequency of front sprung mass
$\omega_{n,r}=2\pi f_{n,r}$	Angular natural frequency of rear sprung mass
$k_{2,f} = \omega_{n,f}^2 m_{2,f}$	Front suspension rate
$k_{2,r} = \omega_{n,r}^2 m_{2,r}$	Rear suspension rate
$\zeta_{2,f}$	Front suspension damping ratio
$\zeta_{2,r}$	Rear suspension damping ratio
$c_{2,r} = 2 k_{2,r} \zeta_{2,r} / \omega_{n,r}^2$	Damping coefficient of front suspension
$c_{2,r} = 2 k_{2,r} \zeta_{2,r} / \omega_{n,r}^2$	Damping coefficient of rear suspension
$k_{1,r} = m_{1,r}\omega_{n,r}^2 - k_{2,r}$	Front tire rate
$k_{1,r} = m_{1,r}\omega_{n,r}^2 - k_{2,r}$	Rear tire rate
l	Wheelbase
$l_f = (l\, m_{2,f}) / (m_2)$	Distance from CG to the rear end
$l_r = (l\, m_{2,f}) / (m_2)$	Distance from CG to the front end
i	Radius of gyration
Z	Vertical displacement at CG
φ	Angular rate about CG

As shown in Table 1, the different front and rear suspension stiffnesses are obtained by changing natural frequency of front and rear sprung masses. Also, the different damping coefficients are obtained by changing front and rear damping ratios.

2.2. Mathematical Modeling

In the half car model given in Fig.1, there is a difference between excitations acting on the front and rear axles. The amplitude of excitation acting to the rear wheel is the same as that of the front wheel, however excitation acting

to the rear wheel is considered to act at the time later. The time (□t) is the function of the vehicle speed and wheelbase. Also, it is described as a ratio of the wheelbase to the forward speed of vehicle. This ratio (l/v) is the time needed to travel a distance that is equal to the wheelbase [8, 11, 12]. Thus, the difference between front and rear excitations as follows:

$$h_f(t) = h_r(t + \Delta t) \tag{5}$$

In this study, the effects of different pitch and bounce center locations on dynamic wheel load oscillations are evaluated with frequency responses. In general, for the frequency response, the sinus wave is applied to the input as test signal. The output of the system excited with sinus wave is also a sinus wave, but it has different amplitude and phase. Therefore, a particular version of dynamic response is built by measuring output magnitude of the system over a range of the input frequencies of sine wave. Therefore, the the front and rear excitations are given as the following:

$$h_f(t) = b\ sin(\omega t) \tag{6}$$

$$h_r(t) = b\ sin(\omega t + \omega l / v) \tag{7}$$

where ω is angular frequency of road. The second term in Eq. (3) shows the phase of responses to the rear input. Under these excitations, in order to achieve the dynamic equations of the half car model for four generalized coordinates, which are vertical displacements ($z_{2,f}$, $z_{2,r}$, $z_{1,f}$, $z_{1,r}$), the energy equations are calculated. Therefore, kinetics energy for the sprung and unsprung mass is as follows:

$$Ek = 0.5(m_2(\dot{z}_{2,f} + (\dot{z}_{2,r} - \dot{z}_{2,f})\, l_f / l)^2 + m_2 i^2((\dot{z}_{2,r} - \dot{z}_{2,f}) / l)^2 + m_{1,f}\, \dot{z}_{1,f}{}^2 + m_{1,r} \dot{z}_{1,r}{}^2) \tag{8}$$

As shown in Eq.(4), in this model, the vertical displacements of vehicle body during bounce motion are described with the front and rear vertical displacements of sprung mass as seen in first term of Eq.(4).

$$z = z_{2,f} + \frac{(z_{2,r} - z_{2,f})}{l} l_f \tag{9}$$

The angular displacements of vehicle body during pitch motion are described in second term of Eq.(8) as follows:

$$\varphi = \frac{z_{2,r} - z_{2,f}}{l} \tag{10}$$

Therefore, the coupling is obtained by substituting Eq.(10) into Eq.(9) as follows:

$$z = z_{2,f} + \underbrace{\frac{(z_{2,r} - z_{2,f})}{l}}_{\varphi} l_f = z_{2,f} + \varphi l_f \tag{11}$$

In this way, when the basic vehicle parameter such as wheelbase is kept constant, only if the spring stiffness and damping coefficients are changed, the pitch motion is coupled to bounce motion.

The equation of the elasticity energy stored in suspension spring and tire spring is written as

$$E_p = 0.5(k_{2,f}(z_{2,f} - z_{1,f})^2 + k_{2,r}(z_{2,r} - z_{1,r})^2 + k_{1,f}\ z_{1,f}{}^2 + k_{1,r}\ z_{1,r}{}^2) \tag{12}$$

The equation of the energy dissipated in absorbers in terms of is written as

$$Ed = 0.5(c_{2,f}(\dot{z}_{2,f} - \dot{z}_{1,f})^2 + c_{2,r}(\dot{z}_{2,r} - \dot{z}_{1,r})^2 \tag{13}$$

These energy equations and jacobian matrices, which are given in the Appendix A, are used for calculating motion equations. Eqs. (8) and (13) are differentiated in terms of the vertical speed of sprung and unsprung masses and Eq.(12) is differentiated with respect to vertical displacements z2,f, z2,r, z1,f, z1,r. by using these jacobian matrices. Therefore, the mass M, stiffness K and damping C matrices are obtained. The mass matrix [M] can be derived as follows:

$$\mathbf{M} = \begin{bmatrix} m_2\left(\frac{l_r}{l}\right)^2 + \frac{m_2 i^2}{l^2} & m_2\left(\frac{l_f l_r}{l^2}\right) - \frac{m_2 i^2}{l^2} & 0 & 0 \\ m_2\left(\frac{l_f l_r}{l^2}\right) - \frac{m_2 i^2}{l^2} & m_2\left(\frac{l_f}{l}\right)^2 + \frac{m_2 i^2}{l^2} & 0 & 0 \\ 0 & 0 & m_{1,f} & 0 \\ 0 & 0 & 0 & m_{1,r} \end{bmatrix}$$

Damping and stifness matrices are as follows:

$$\mathbf{C} = \begin{bmatrix} c_{2,f} & 0 & -c_{2,f} & 0 \\ 0 & c_{2,r} & 0 & -c_{2,r} \\ -c_{2,f} & 0 & c_{2,f} & 0 \\ 0 & -c_{2,r} & 0 & c_{2,r} \end{bmatrix}$$

$$\mathbf{K} = \begin{bmatrix} k_{2,f} & 0 & -k_{2,f} & 0 \\ 0 & k_{2,r} & 0 & -k_{2,r} \\ -k_{2,f} & 0 & k_{1,f} + k_{2,f} & 0 \\ 0 & -k_{2,r} & 0 & k_{1,r} + k_{2,r} \end{bmatrix}$$

Tire spring stiffness and road excitation matrices are as follows:

$$\mathbf{K_t} = \begin{bmatrix} 0 & 0 \\ 0 & 0 \\ k_{1,f} & 0 \\ 0 & k_{1,r} \end{bmatrix} \qquad \mathbf{h} = \begin{bmatrix} 0 \\ 0 \\ h_{1,f} \\ h_{1,r} \end{bmatrix}$$

As a consequence, the matrix vector equation is written as

$$\mathbf{M\ddot{z} + C\dot{z} + Kz = K_t h} \quad (14)$$

For sinusoidal excitation, the general solutions of the vertical displacements are described as follows:

- $z_{2,f}(t) = z_{2,f(re)} + z_{2,f(im)} = A\sin\omega t + B\cos\omega t$ (15)
- $z_{2,r}(t) = z_{2,r(re)} + z_{2,r(im)} = C\sin\omega t + D\cos\omega t$ (16)
- $z_{1,f}(t) = z_{1,f(re)} + z_{1,f(im)} = E\sin\omega t + F\cos\omega t$ (17)
- $z_{1,r}(t) = z_{1,r(re)} + z_{1,r(im)} = G\sin\omega t + H\cos\omega t$ (18)

where the subscripts *re* and *im* refer to the real and imaginary parts of the vertical displacements for the front and rear suspensions, respectively. The coefficients A,C,E,G and B,D,F,H are real and imaginary parts, respectively as shown Eqs. (15), (16), (17) and (18). Thereby, the magnitudes of vertical motions of sprung and unsprung masses are obtained as follows:

$$\left|z_{2,f}\right| = \sqrt{A^2 + B^2} \quad (19)$$

$$\left|z_{2,r}\right| = \sqrt{C^2 + D^2} \quad (20)$$

$$\left|z_{1,f}\right| = \sqrt{E^2 + F^2} \quad (21)$$

$$\left|z_{1,r}\right| = \sqrt{G^2 + H^2} \quad (22)$$

As a result, in order to determine the magnitudes, the coefficients A,B,C,D,E,F,G,H are calculated by using the matrix equation system as follows:

$$\underbrace{\begin{bmatrix} -\omega^2[\mathbf{M}]+[\mathbf{K}] & \omega[\mathbf{C}] \\ -\omega[\mathbf{C}] & -\omega^2[\mathbf{M}]+[\mathbf{K}] \end{bmatrix}}_{\mathbf{X}} \underbrace{\begin{bmatrix} z_{2,f(re)} \\ z_{2,r(re)} \\ z_{1,f(re)} \\ z_{1,r(re)} \\ z_{2,f(im)} \\ z_{2,r(im)} \\ z_{1,f(im)} \\ z_{1,r(im)} \end{bmatrix}}_{\mathbf{Z}} = \underbrace{\begin{bmatrix} 0 & 0 \\ 0 & 0 \\ 0 & 0 \\ 0 & 0 \\ 0 & 0 \\ 0 & 0 \\ k_{1,f} & 0 \\ 0 & k_{1,r} \end{bmatrix}}_{\mathbf{Y}} \underbrace{\begin{bmatrix} 0 \\ 0 \\ 0 \\ 0 \\ 0 \\ 0 \\ h_{f(im)} \\ h_{r(im)} \end{bmatrix}}_{\mathbf{h}} \quad (23)$$

where **M**, **C**, **K** are mass, stiffness and damping matrices of a half car model. Thereby, the coefficients of real and imaginery parts are calculated as the following:

$$\mathbf{Z = X^{-1} Y\ h} \quad (24)$$

2.3. Modelling of dynamic wheel load oscillations

The wheel load oscillations consist of the static component arising from the weight of vehicle and the dynamic component arising from oscillations as follows:

$$F_z = F_{z,st} + F_{z,dyn} \quad (25)$$

where F_z is the total wheel load, $F_{z,st}$ is the static wheel load and $F_{z,dyn}$ is the dynamic wheel load. The dynamic tire load oscillations show the changes in contact between tire and the road during pitch and bounce motions. It is expressed for front and rear axles as the following:

$$F_{z,dyn(f)} = k_{1,f}(z_{1,f} - h_f(t)) \quad (26)$$

$$F_{z,dyn(r)} = k_{1,r}(z_{1,r} - h_r(t)) \quad (27)$$

In this study, the effects of dynamic wheel load oscillations are investigated by ratio of the dynamic wheel load to the static wheel load. For this, the dynamic tire load oscillations of the front axle as follows:

$$\left|F_{z,dyn(f)}\right| = k_{1,f}(E\cos\omega t + F\sin\omega t - b\sin\omega t) \quad (28)$$

Thus, the amplitude ratio of the dynamic tire load oscillations are calculated for the front axle as follows:

$$\left|\frac{F_{z,dyn(f)}}{F_{z,st(f)}}\right| = \frac{k_{1,f}\sqrt{E + (b+F)^2}}{F_{z,st(f)}} \quad (29)$$

Also, the dynamic tire load oscillations of the rear axle are calculated as follows:

$$\left|F_{z,dyn(r)}\right| = k_{1,r}([G\cos\omega t + H\sin\omega t] - [b\sin(\omega t + \omega l/v)]) \quad (30)$$

As the excitation of road surface is a function of wheelbase and vehicle speed for the rear axle, the amplitude ratio of the dynamic tire load oscillations for the rear axle is different from that of front. Thus, the dynamic tire load ratio of the rear axle is obtained as follows:

$$\left|\frac{F_{z,dyn(r)}}{F_{z,st(r)}}\right| = \frac{k_{1,r}\sqrt{(b\cos(\omega l/v)+G)^2 + (b\sin(\omega l/v)+H)^2}}{F_{z,st(r)}} \quad (31)$$

3. RESULTS AND DISCUSSION

In this study, in order to vary locations of oscillation centre and obtain natural frequencies, the following parameters are defined.

$$\alpha = \frac{k_f + k_r}{m_2} \quad (32)$$

$$\beta = \frac{k_f l_f - k_r l_r}{m_2} \quad (33)$$

$$\gamma = \frac{k_f l_f^{\,2} + k_r l_r^{\,2}}{m_2} \quad (34)$$

where k_f is front suspension spring stiffness and k_r is rear suspension spring stiffness. Therefore, the natural frequencies are written for the pitch and bounce motion of the vehicle body as follows:

$$\omega_{1,2} = \sqrt{\frac{(\alpha+\gamma)}{2} \pm \sqrt{\frac{(\alpha-\gamma)^2}{4} + \frac{\beta^2}{k^2}}} \quad (35)$$

These natural frequencies are related to vertical motions and angular motions about pitch and bounce oscillation centres. As a result, the position of oscillation centres is calculated as follows:

$$\frac{z}{\phi_1} = -\frac{\beta}{(\alpha - \omega_1^2)} \tag{36}$$

$$\frac{z}{\phi_2} = -\frac{\beta}{(\alpha - \omega_2^2)} \tag{37}$$

These ratios describe the distance from CG to oscillation centres of pitch and bounce. The ratio has two modes. One of them is for pitch motion and the other is for bounce motion. When the ratio is positive, both *z* and φ must be positive and negative. Thus, oscillation center will be ahead of CG by distance z/φ. Likewise, the oscillation center will be behind of CG for the root with negative value. Therefore, one distance falls outside the wheelbase, and the other distance falls within wheelbase. When the centre is outside wheelbase, the motion is predominantly bounce, and the related frequency is natural frequency of the bounce. When the centre is within wheelbase, the motion is pitch, and the related frequency is pitch frequency [12].

In order to observe the effects of the changes in location of oscillation centre on the compromise between ride comfort and safety, the pitch stiffness and the damped natural frequencies of pitch and bounce are used. For the frequencies, it is considered Olley's flat ride condition that the pitch frequency is 1.2 times higher than bounce frequency. For this, the damped natural frequencies of pitch and bounce are calculated as follows:

$$f_{b(d)} = \frac{\omega_1}{2\pi}\sqrt{(1-\zeta_b)^2} \tag{38}$$

$$f_{p(d)} = \frac{\omega_2}{2\pi}\sqrt{(1-\zeta_p)^2} \tag{39}$$

where ζ_b is bounce damping ratio and ζ_p is pitch damping ratio. In this study, tyre damping is neglected, compared with the damper damping. For this reason, the equivalent damping for front and rear axle is equal to damping coefficients of individual front and rear dampers, respectively. Thereby, the damping ratios for pitch and bounce are expressed as follows:

$$\zeta_b = \frac{c_{2,f} + c_{2,r}}{\sqrt{m_2(k_f + k_r)}} \tag{40}$$

$$\zeta_p = \frac{c_{2,f} + c_{2,r}}{i\sqrt{m_2(k_f + k_r)}} \tag{41}$$

Also, in order to asses the compromise between ride safety and comfort of pitch with respect to pitch stiffness, it is considered that the pitch ride improves, as the effective pitch stiffness decreases. The pitch stiffnesses with spring stiffness is as follows:

$$k_p = k_f l_f^{\,2} + k_r l_r^{\,2} \tag{42}$$

3.1. Frequency Responses

In order to evaluate the coupling effect between pitch and bounce motions on dynamic wheel load oscillations through different locations of oscillation centers, the frequency responses of front and rear dynamic wheel load oscillations are obtained by using Eqs. (29) and (31). The different oscillation centre locations are obtained by changing the front and rear suspension stiffnesses using Eqs.(36) and (37). In here, the stiffnesses are derived from the natural frequencies of front and rear suspension as shown in Table 1. Therefore, the different oscillation centers are obtained by changing only spring stiffnesses through natural frequencies as follows:

- The natural frequency of front ($f_{n,f}$) is lower than that of rear suspension ($f_{n,r}$)
- The natural frequency of front ($f_{n,f}$) is higher than that of rear suspension ($f_{n,r}$)

The trade off analysis was carried out to determine optimum natural frequency and damping coefficient with Ride Comfort Index (RCI) and Road Holding Index (RHI) as shown in Fig. 2.

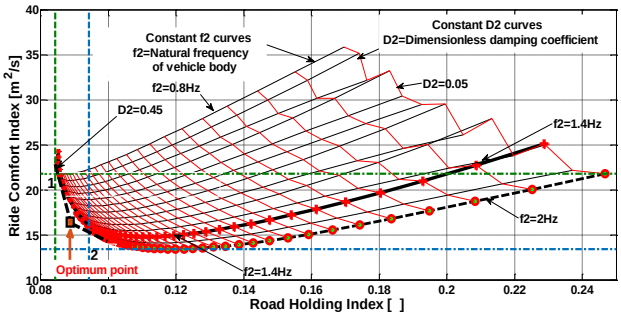

Figure 2. Trade off analysis diagram for ride comfort and road holding

The ratio of requency weighted vertical acceleration of vehicle body to vehicle speed is computed for RCI and standard deviation of dynamic wheel load is obtained for RHI by considering different natural frequencies front and rear sprung masses of half car model and dimesionless damping coeffcient of front and rear dampers with vehicle speeds 10, 20 and 35m/s. The ranges $0.8\text{Hz}<f_2<2\text{Hz}$ and $0.05<D_2<0.45$ are considered for the natural frequency and the damping coefficient, respectively. In Fig. 2, it is considerable point that the smaller the driving comfort index and the road holding index, the better comfort and handling are achieved.

In Fig.2, 1 and 2 represent the points to provide the best road holding and ride comfort, respectively. Thus, it seems that the optimum point lies between these two points. To determine the natural frequency and damping rate determining the optimum point, the constant natural frequency and damping rate curves approaching the optimum point were determined as shown in Fig.2. In this way, it is clearly seen that the natural frequency and damping coefficient are 1.4 Hz to 0.45, which provides

the best handling without worsening driving comfort. At the same time, the natural frequency of 2Hz seems to worsen the handling slightly, despite the better comfort. As a result, it was determined that the frequency range that provides the best handling without deteriorating comfort at the point where the optimum point is located is between 1.4 Hz and 2 Hz with 0.45 damping coefficient. For this reason, in this study, 1.4 Hz and 2 Hz are considered for the natural frequencies of sprung masses $m_{2,f}$ and $m_{2,r}$ and 0.45 is taken into account for front and rear dampers.

3.1.1. Material and methods for frequency responses

All frequency response results are evaluated for the forward speeds of vehicle 10, 20, 35m/s with the dynamic index (i^2 /l_f l_r)=0.8 according to Olley's modern car criteria. This dynamic index describes the coupling between vertical displacement modes of the front and rear suspension.

When Eqs. (34**)**, (35) and (36) are considered, it is clearly seen that the positions of vehicle body CG within wheelbase are important factor affecting the location of oscillation center as seen in Eqs.(9), (10) and (11). Thereby, the results are analyzed with respect to the different positions of CG for different front and rear axle loads as follows:

- The CG is close to front suspension for higher front axle loads than that of rear.
- The CG is close to rear suspension for higher rear axle loads.

Also, the location of oscillation center is calculated by taking CG of vehicle body as a reference as shown in Table 2 and 4. In Table 2 and 4, the negative value shows that the oscillation center moves to backward of CG. Also, positive values indicate that the oscillation center moves to forward of CG. In here, it is cearly seen that bounce center is at outside of wheelbase and pitch center is within wheelbase.

Therefore, the effects of the changes in coupling effect on dynamic wheel load oscillations are investigated with different oscillation center locations through suspension spring stiffness and the location of CG within wheelbase. The results are compared for different forward speeds of vehicle and positions of the CG. Also, the compromise between ride comfort and ride safety is analyzed relative to the pitch stiffness and the ratio of pitch natural frequency to that of bounce. For this, firstly, the locations of oscillation centers are determined.

3.1.2. Determination of location of pitch and bounce centers

A road excitation acting on the front or rear wheel induce a moment about each oscillation center, and it will excite both bounce and pitch oscillations. Thus, the vehicle body motion will be the sum of the oscillations about the two centers during pitch motion [8]. The sum varies according to location of the centers. As the bounce center moves away, the angular oscillation of pitch motion will be met with vertical diplacement of bounce. In this way, the angular motion of pitch will be converted to vertical motion. This will reduce the level of angular oscillation. For this reason, the effects of locations of oscillation centers on dynamic wheel load oscillations should be considered. For this, firstly the locations of oscillation centers are described as shown in Fig.3.

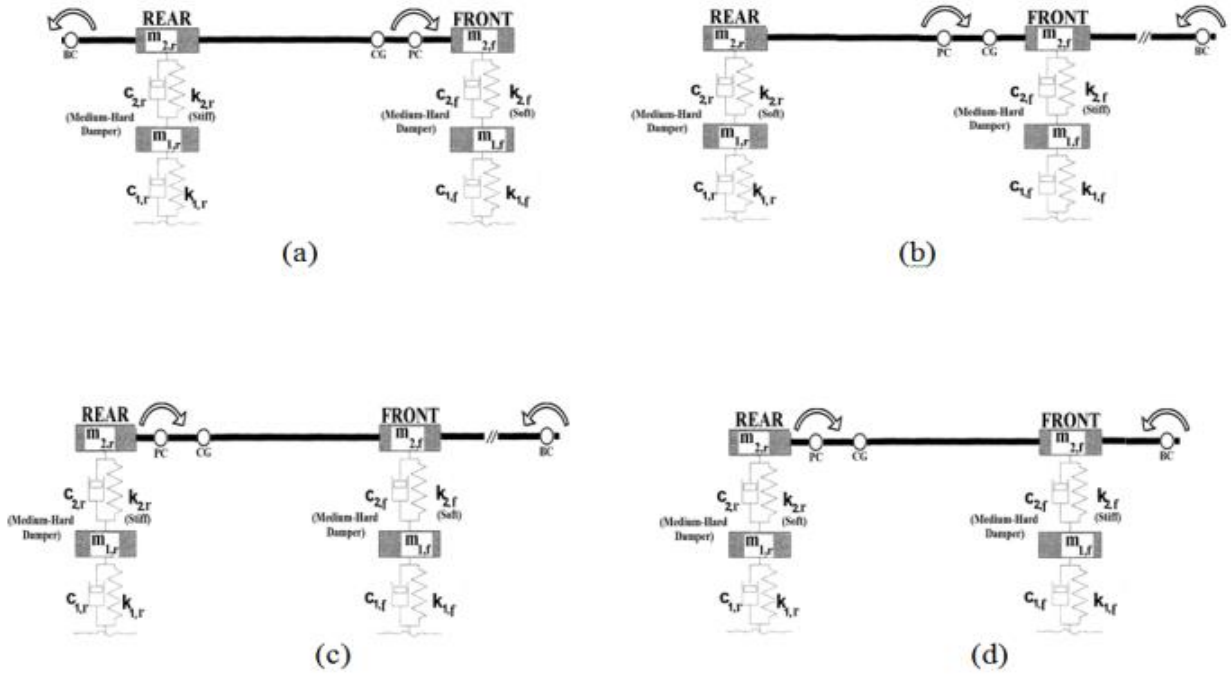

Figure 3. The location of pitch and bounce centers for cases 1 and 2

The Fig.3 shows the locations of pitch and bounce centers according to CG for the vehicle pitching to forward, where PC, BC and CG describe pitch center, bounce center and center of gravity, respectively. Fig.3a shows the location of oscillation centers for the vehicle which has a harder rear suspension and forward CG. Fig.3b shows the location of oscillation centers for the vehicle which has a harder front suspension and forward CG. Fig.3c shows the location of oscillation centers for the vehicle which has a harder rear suspension and backward CG. Fig.3d shows the location of oscillation centers for the vehicle which has a harder front suspension and backward CG.

repectively. As shown in Table 2, when the rear suspension spring is set to harder with forward CG as shown in Fig.3a, the bounce center is 3.2146m to left side of CG. Also, the pitch oscillation center is 0.46m to right side of the CG as shown in Fig.3a. When the front suspension spring is set to harder with same positon of CG, the bounce center moves 8.6422m to right side of the CG as shown in Table 2.

Also, when the front suspension spring is set to harder with backward CG as shown in Fig 3c, the bounce center moves 2.98m to right side of the CG and pitch center moves 0,4182m to left side of CG as shown in Table 2.The results indicate that bounce moves toward to

Table 2. The ride comfort parameters and the location of oscillation centers for Case1

l_f= 1.5m – l_r=2m							
Conditions	$f_{b(d)}$ [Hz]	$f_{p(d)}$ [Hz]	$f_{p(d)}/f_{b(d)}$ -	z/φ-*bounce* [m]	z/φ-*pitch* [m]	k_p [Nm/ degree]	c_p [Nms/ degree]
f_f=1.4Hz < f_r=2Hz	1.0648	2.0708	1.9448	-3.2146	0.4666	5.5558	0.3320
f_f=2Hz > f_r=1.4Hz	1.1845	1.8742	1.5823	8.6422	-0.1736	3.4529	0.2341
l_f= 2.5m – l_r=1m							
f_f=1.4Hz < f_r=2Hz	1.1593	2.0278	1.7429	5.4845	-0.2279	1.4739	0.0887
f_f=2Hz > f_r=1.4Hz	0.9338	2.4514	2.6251	2.9891	-0.4182	1.0001	0.0667

Also, the pitch oscillation center moves 0.1736m to left side of the CG as shown in Fig.3a. This shows that position of bounce center is at outside of rear and front axles and pitch center lies between front and rear axles with this suspension setting of forward CG. Also, the results indicate that bounce moves toward to hard suspension spring and pitch center moves to opposite side of hard spring with forward CG. However, when the rear suspension spring is set to harder with backward CG as shown in Fig 3c, the bounce center moves 5.48m to opposite direction of CG and pitch center moves 0,2279m to left side of CG as shown in Table 2. The pitch oscillation center is 0.1736m to left side of the CG as shown in Fig.2a.

3.1.3. Frequency responses for case 1

From point of view of above information, the frequency responses are investigated for case 1as shown in Fig.4. In here, the results are evaluated according to different location of CG for same suspension settings. Also, these results are assessed according to different suspension stiffness at same location of CG as shown in Fig.4.

It is clearly seen that the changes in location of oscillation center have effect on dynamic wheel load oscillations at the resonance areas of vehicle body and axle. In this way, Fig.4 shows that the dynamic load oscillations can be reduced by making the suspension spring harder at same position of CG.

Therefore, the dynamic load oscillations of rear wheel are reduced with harder front suspension at resonance area of vehicle body, regardless of changes in CG.

The exact location of oscillation centers is determined as shown in Table 2. Table 2 shows the calculated parameters for case 1. In table 2, the positive and negative signs represent movement to right and left sides, opposite side of hard suspension spring and pitch center moves to same direction as hard spring with backward CG. Therefore, the effect of harder front or rear suspension springs on location of pitch and bounce center depends greatly on position of CG. Hard springs cause bounce center to lie outside wheelbase. Also, the pitch center lies inside wheelbase with harder springs. Thus, harder rear suspension moves bounce and pitch centers to opposite side of CG. However, harder front suspension only translates both of two centers to left or right side at same direction.

However, the same improvement on rear axle is obtained at axle resonance area by using harder rear suspension at both positions of CG.

The dynamic load oscillations of front axle are reduced with harder rear suspension at vehicle body resonance area. In spite of this, same improvement is achieved at axle resonance area by using harder front suspension. These improvements can vary according to increases in vehicle speed. Hence, the sensivity of oscillations decreases against the increases in vehicle speed with improvement at vehicle body resonance area as shown in Fig.3, whereas this sensivity greatly increases at axle resonance area. This shows that it is more difficult to damp the oscillations at high frequencies as the vehicle speed increases.

On the other hand, the oscillations are able to be reduced by changing position of CG with same suspension settings. Thus, the improvement on dynamic load oscillations of rear wheel continues at vehicle body resonance area, even if CG moves toward to rear axle.

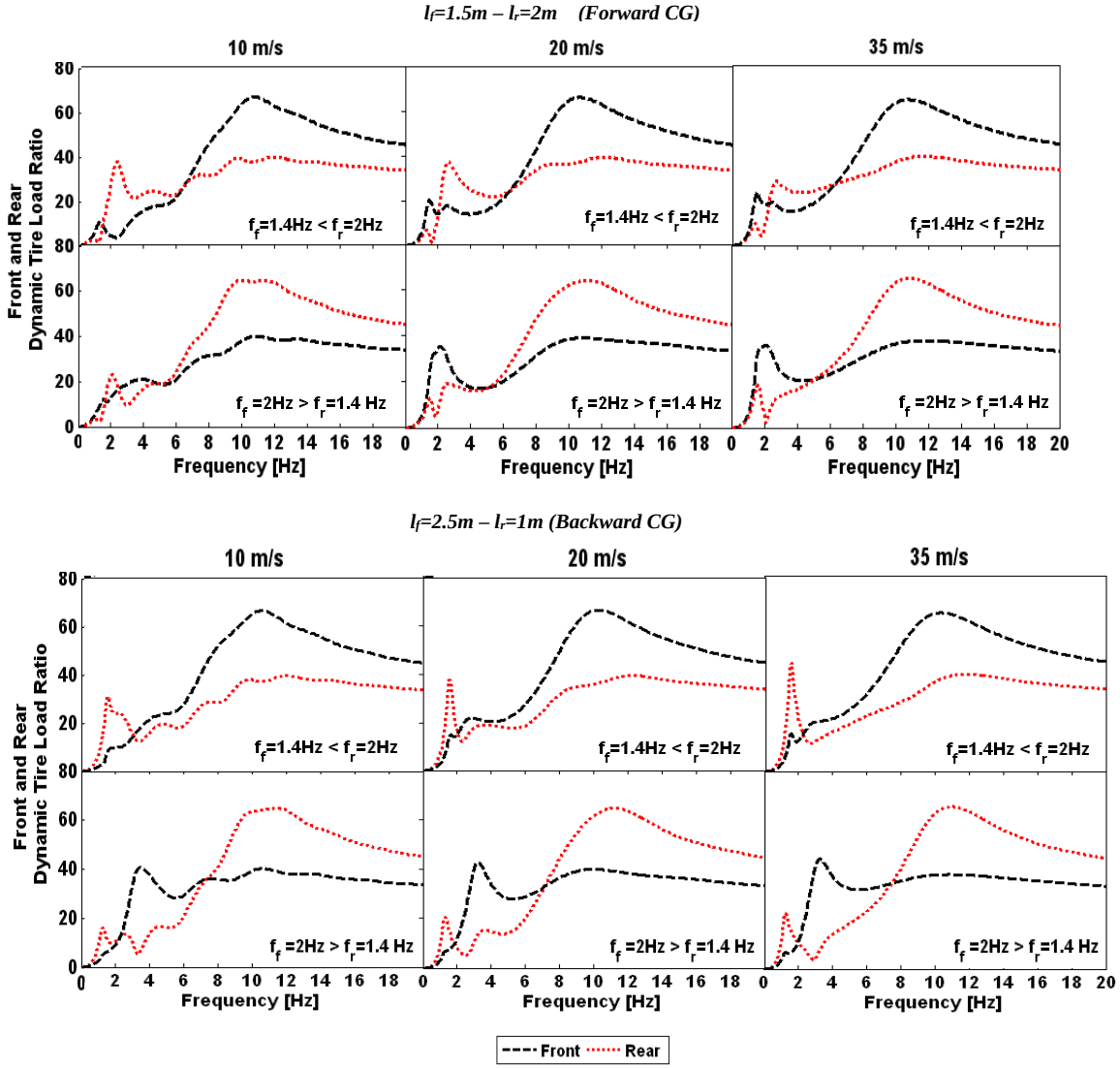

Figure 4. The frequency responses for Case 1

These results indicate that the dynamic load oscillations of rear wheel are reduced at by moving the bounce center to outside of front axle irrespective of position of pitch center and CG, when the wheels are excited by road roughness which has vehicle body resonance frequency such as rough terrain. Also, the rear axle oscillations are reduced by moving bounce center to opposite side of pitch and CG, when rear axle is excited at resonance frequency of axle such as smoother road. The front dynamic load oscillations are greatly reduced at vehicle body resonance area with movement of bounce center to opposite side of pitch center and CG.

Also, the improvement on dynamic load oscillations of front wheel continues, as long as CG moves toward to front axle. However, the changes in position of CG have not any effect on these improvements at axle resonance area.

At same time, the front oscillations are decreased by moving bounce center to outside of front axle irrespective of position of pitch center and CG Moreover, the frequency ratio and pitch stiffness are investigated to determine the most convenient location of oscillation centers according to the best ride comfort. Therefore, the lowest pitch stiffness and frequency ratio are obtained with harder front suspension for vehicle with forward CG. As for vehicle with backward CG, the lowest pitch stiffness is achived with harder front suspension and the lowest frequency ratio is obtained with harder rear suspension. All results are summarized as shown in Table 3.

Table 3. The investigation results for case 1

Conditions	Location of CG	Movement of Oscillation Centers	Improvement On Dynamic Wheel Loads for Axles	Improvement Level	Comfort	Sensivity to Vehicle Speed
If $f_{n,f}<f_{n,r}$ with $D_f=D_r$	Forward	BC to rear side of rear axle PC to front side of CG	Front at VBRF Rear at ARF	High Very High	Very Low	High Very Low
If $f_{n,f}>f_{n,r}$ with $D_f=D_r$	Forward	BC to front side of front axle PC to rear side of CG	Rear at VBRF Front at ARF	Very Low Very High	Low	Very Low Very Low
If $f_{n,f}<f_{n,r}$ with $D_f=D_r$	Backward	BC to front side of front axle PC to rear side of CG	Front at VBRF Rear at ARF	Very High Very High	High	High Very Low
If $f_{n,f}>f_{n,r}$ with $D_f=D_r$	Backward	BC to front side of front axle PC to front side of front axle	Rear at VBRF Front at ARF	Very High Very High	Very High	Low Very Low

*VBRF: Vehicle Body Resonance Frequency - *ARF: Axle Resonance Frequency

As a result, both pitch and bounce motions of vehicle body should be encountered with hard front suspension to reduce the front and rear wheel load oscillations with forward CG. This can be achieved with same front and rear damping capacities. Nevertheless, in order to reduce both of load oscillations of vehicle which has a backward CG, it is clearly seen that the damping capacities need to be changed.

3.1.4 The frequency responses for Case 2

In Case 1, the damping of damper was kept constant. In case 2, the damping ratio is changed with the first and second condition of case 1. The results are given in Fig.5 and Table 4 for the first condition of Case 2. Also, the locations of the oscillation centers are given in Fig.5 for the first and second conditions of case 2.

Also, the further improvement may be obtained for the vehicle, which has a forward CG, by changing the front and rear damping capacities. For this reason, the damping capacities of front and rear suspension should be changed for same location of oscillation center according to CG of vehicle body. For this, case 2 is considered for two different conditions.

Thereby, as shown in Table 4, the locations of bounce and pitch oscillation centers with stiffer front damper are same as that of harder rear damper for same location of CG. Because only suspension stiffness can change the location of oscillation centers according to Eqs. (33), (34) and (35).

Table 4. The ride comfort parameters and the location of oscillation centers for the first condition of Case 2

Conditions f_f=1.4Hz –f_r=2Hz	$f_{b(d)}$ [Hz]	$f_{p(d)}$ [Hz]	$f_{p(d)}/f_{b(d)}$ -	z/φ-bounce [m]	z/φ-pitch [m]	k_p [MNm/degree]	c_p [MNms/degree]
			l_f= 1.5m – l_r=2m				
D_{2f}=0.25 -D_{2r}=0.45	0.6842	1.7011	2.4862	-3.2146	0.4666	5.5585	0.5958
D_{2f}=0.45 -D_{2r}=0.25	0.8333	1.9528	2.3433	-3.2146	0.4666	5.5585	0.3338
			l_f= 2.5m – l_r=1m				
D_{2f}=0.25 -D_{2r}=0.45	0.7499	1.9321	2.5937	5.4845	-0.2279	1.4739	0.1547
D_{2f}=0.45 -D_{2r}=0.25	0.9073	1.4376	1.5845	5.4845	-0.2279	1.4739	0.0938

In this way, when the Fig. 5 is considered by taking Fig. 3a and 3b as a reference, the harder front damper considerably reduces both front and rear wheel oscillations with harder rear suspension at resonance area of axle for all CG positions. In addition, the further improvement is achieved by increasing vehicle speed as shown in Fig.5.

In here, it is remarkable point that bounce motion of vehicle body should be encountered with harder damper to quickly respond to the pitching moment. In this way, the increases in vehicle speed enable the oscillations to be more effectivelty damped. The results of the second condition are given in Fig.5 and Table 5.

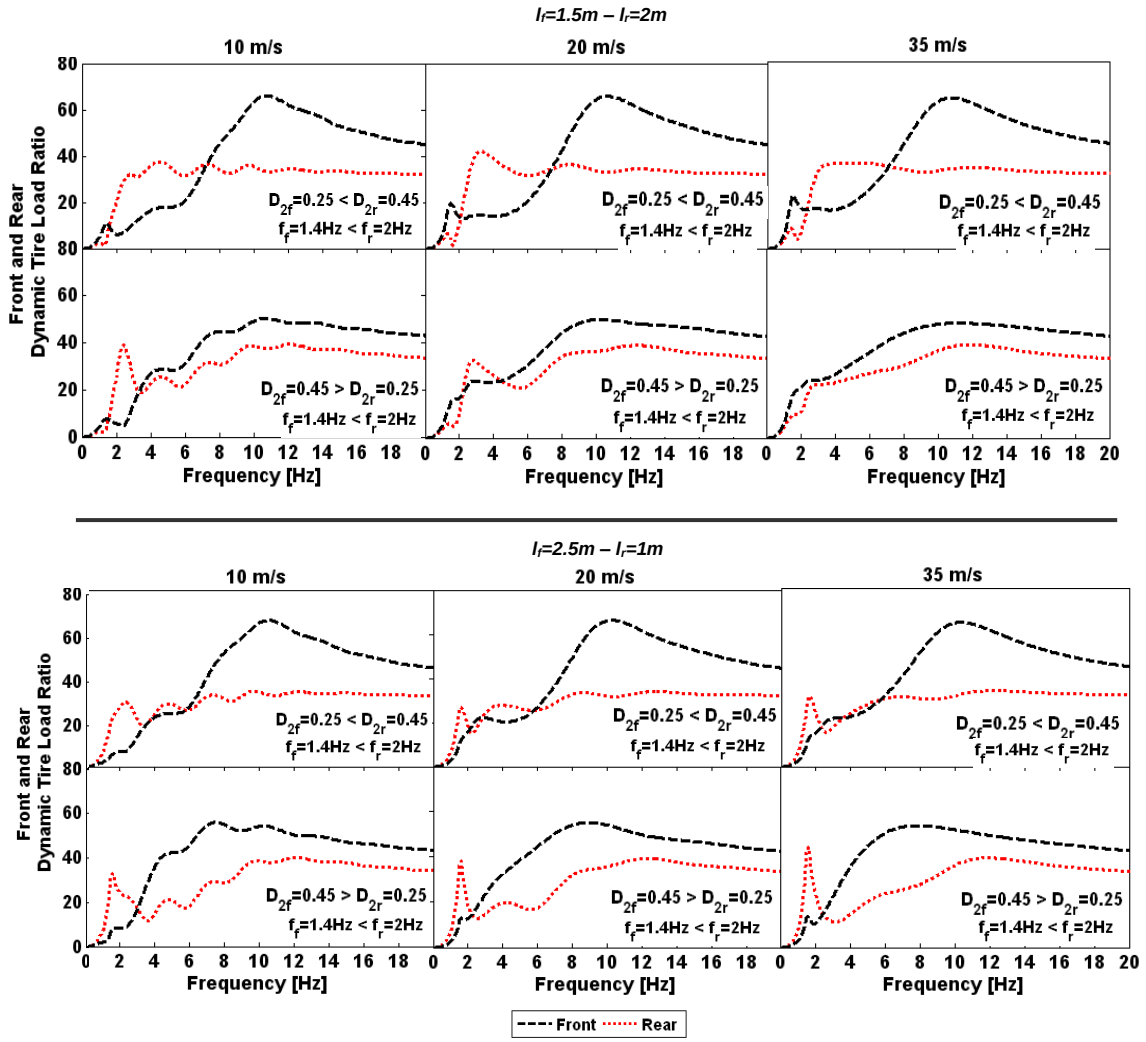

Figure 5. The frequency responses for the first condition of Case 2

Table 5 shows that the locations of bounce and pitch oscillation centers with different damping ratios are same. Therefore, when Fig. 6 is considered with reference of Figs. 3c and 3d, the increases in damping capacity of rear damper enable the front and rear wheel load oscillations to be considerably reduced with harder front suspension at resonance areas of axle.

Table 5. The ride comfort parameters and the location of oscillation centers for the second condition of Case 2

Conditions f_f=2Hz –f_r=1.4Hz	$f_{b(d)}$ [Hz]	$f_{p(d)}$ [Hz]	$f_{p(d)}/f_{b(d)}$ -	*z/φ-bounce* [m]	*z/φ-pitch* [m]	k_p [MNm/ degree]	c_p [MNms/ degree]
l_f= 1.5m – l_r=2m							
D_{2f}=0.25 -D_{2r}=0.45	0.9270	1.6545	1.7847	8.6422	-0.1736	3.4519	0.4187
D_{2f}=0.45 -D_{2r}=0.25	0.7611	1.7064	2.2419	8.6422	-0.1736	3.4519	0.2367
l_f= 2.5m – l_r=1m							
D_{2f}=0.25 -D_{2r}=0.45	0.7308	2.3766	3.2519	2.9891	-0.4182	1.0001	0.1129
D_{2f}=0.45 -D_{2r}=0.25	0.6001	1.3399	2.3330	2.9891	-0.4182	1.0001	0.0739

As a result, in Figs. 5 and 6, it is remarkable point that the changes in damping capacity have effect on wheel load oscillations at especially resonance area of the axle. In this area, the dyanmic wheel loads are considerably reduced by varying the damping cpacities according to the suspension spring stiffnesses .

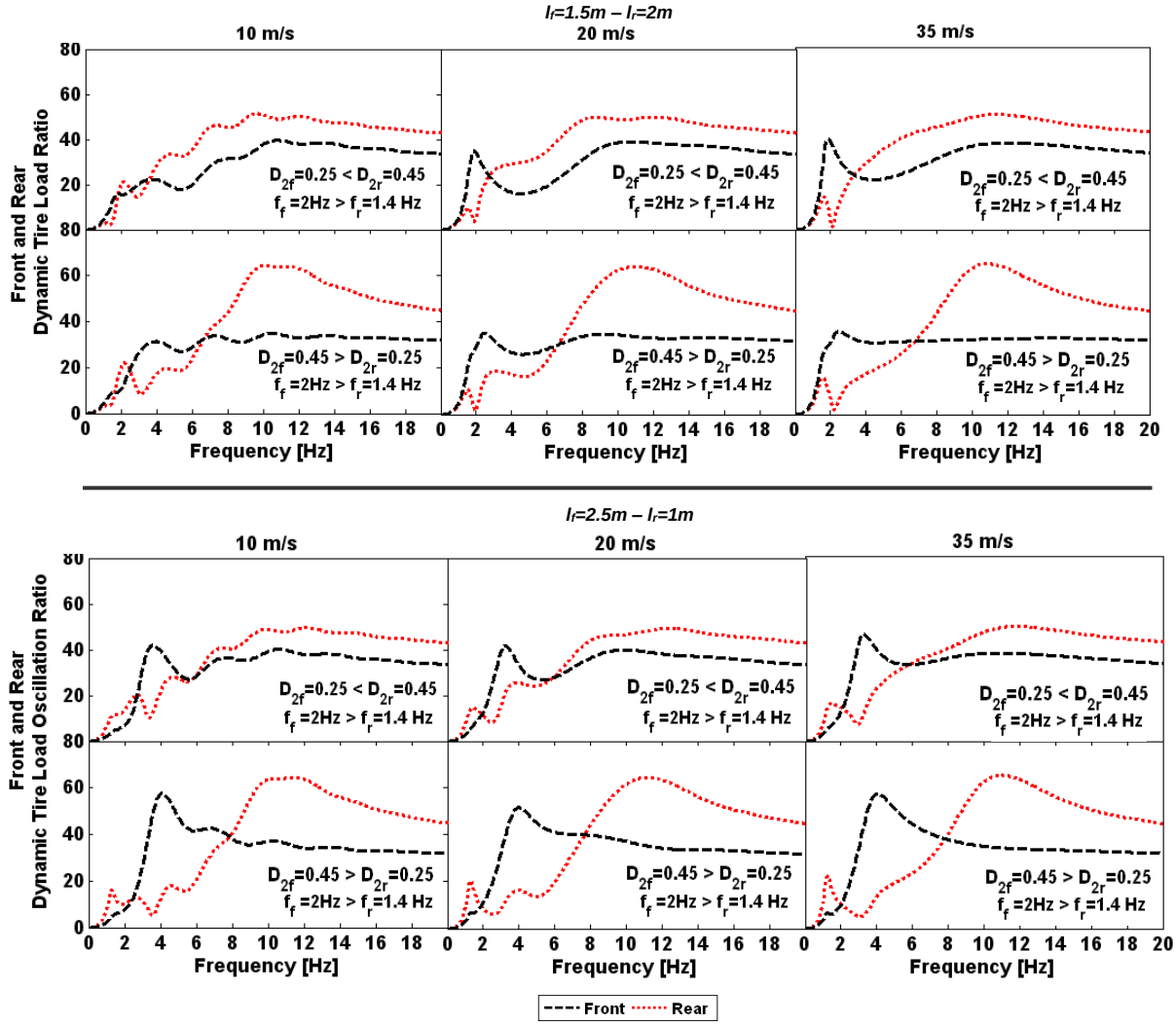

Figure 6. The frequency responses for the second condition of Case 2

3.1.5. The ride comfort and suspension stroke analysis

In the frequency analysis realized in the previous section, it is seen that the dynamic wheel load oscillations can be reduced with the oscillation center changes and the oscillation center positions that can reduce the dynamic wheel load oscillations can also be determined. Improvements in dynamic wheel load may be expected to worsen driving comfort. The reasons of this deterioration are clearly seen in the trade off diagram given in Figure 2. Therefore, it is necessary to analyze the effects of the oscillation center changes, which correct dynamic wheel load oscillations, on driving comfort. For this, the frequency analysis of the acceleration amplitudes of the bounce and pitch motions is performed as shown in Figure 7. As shown in Figure 7, as vehicle speed increases, the vehicle body is exposed to less acceleration at wider intervals. This indicates that the maximum acceleration occurs more slowly as the vehicle speed increases. On the other hand, pitch and bounce acceleration amplitudes occur more frequently as vehicle speed decreases.

In here, it was considered that acceleration level of pitch will decrease, when angular acceleration level of pitch is lower than that of bounce.

Because, the angular oscillation of pitch motion will be more met with more vertical diplacement of bounce and thus, the gerater part of angular motion will be converted into vertical motion. This will provide the ride comfort. Therefore, the pitch acceleration amplitudes remained below the bounce acceleration amplitudes in all frequency ranges. This clearly shows that the developed method does not worsen ride comfort regardless of the change in vehicle speed. Also, all results show that the better ride comfort is achieved as the vehicle speed increases. On the other hand, the ride comfort is relatively reduced in vehicle speed of 10m/s since the pitch acceleration amplitude is higher than that of the bounce at very low frequency road inputs. For this reason, the ride comfort relatively deteriorates, since the road inputs are slightly met by angular motion of vehicle body in this frequency range.

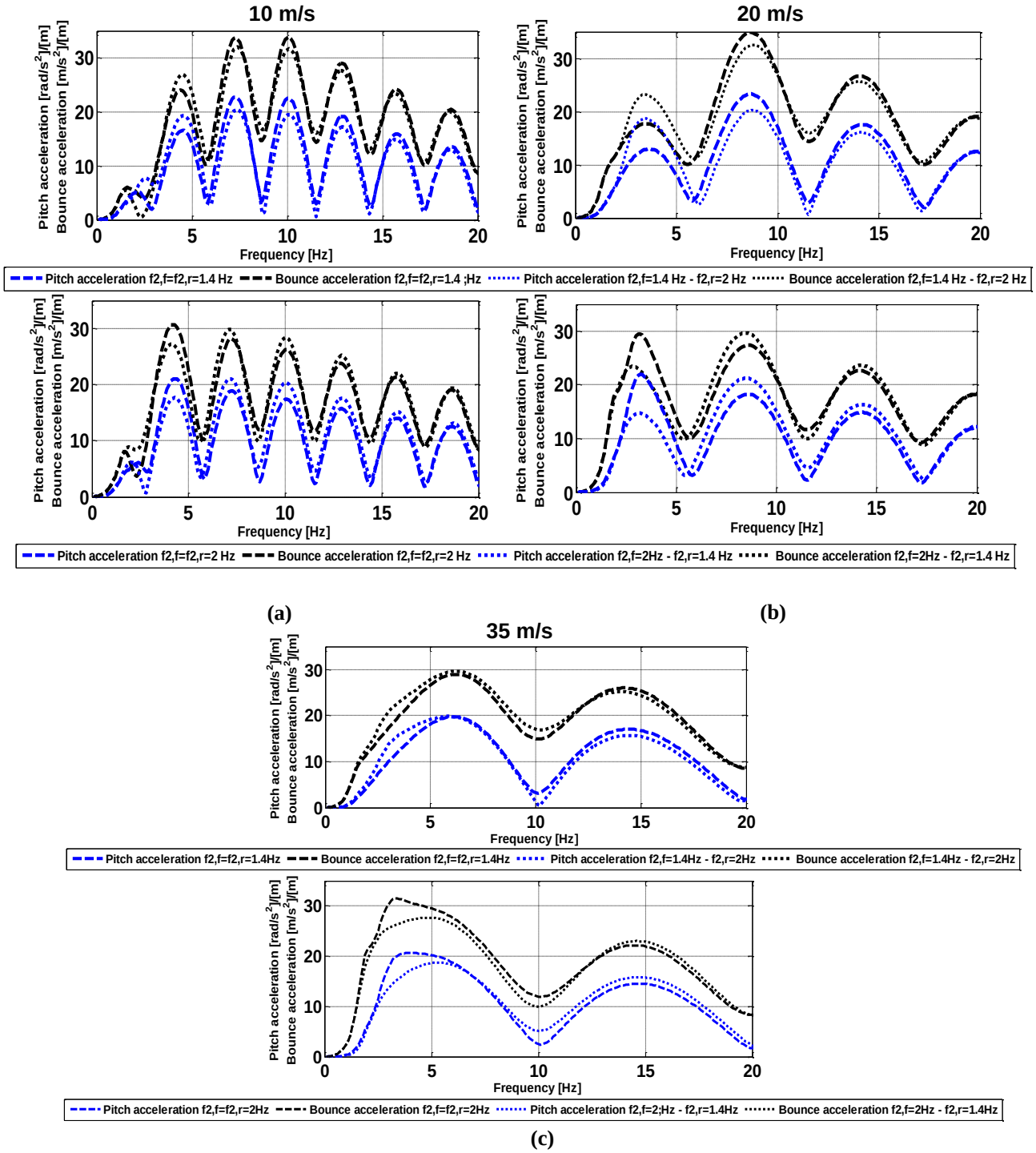

Figure 7. Angular acceleration of pitch and vertical acceleration of bounce

The improvements on ride comfort can be achieved with sufficient suspension spring displacement. In other words, as spring displacement increases, its contribution to ride comfort will increase, since the spring will absorb more road input. The spring displacement can be achieved with suspension stroke. The more compression or expansion of the suspension relative to the road input, the more the spring displacement will increase and the spring will be able to dampen the more road input.

For this reason, the contribution of the suspension stroke to the ride comfort should be determined according to the oscillation center changes. For this, the front and rear suspension strokes are investigated according to location of oscillation centers as shown in Fig.8. In Fig.8, the difference between the displacements of sprung and unsprung masses is inveastigated. In here, the road input is applied to front and rear wheels as sinusoid which has height of 0.050m.

In this way, the changes in suspension stroke are determined according to the frequency of road input. In Fig.8, the positive and negative signs represent compression and expansion, respectively. As shown in Fig.8, the frequencies at which the front and rear suspension spring oscillations occur differ according to each other.

While the rear suspension stroke oscillations occur at very low frequencies, the occurring of the front suspension stroke oscillations completely depend on spring stiffness of front and rear suspension. Also, regardless of vehicle speed, suspension stroke oscillations increase at low frequencies, whereas the oscillations decrease significantly as the frequency increases.

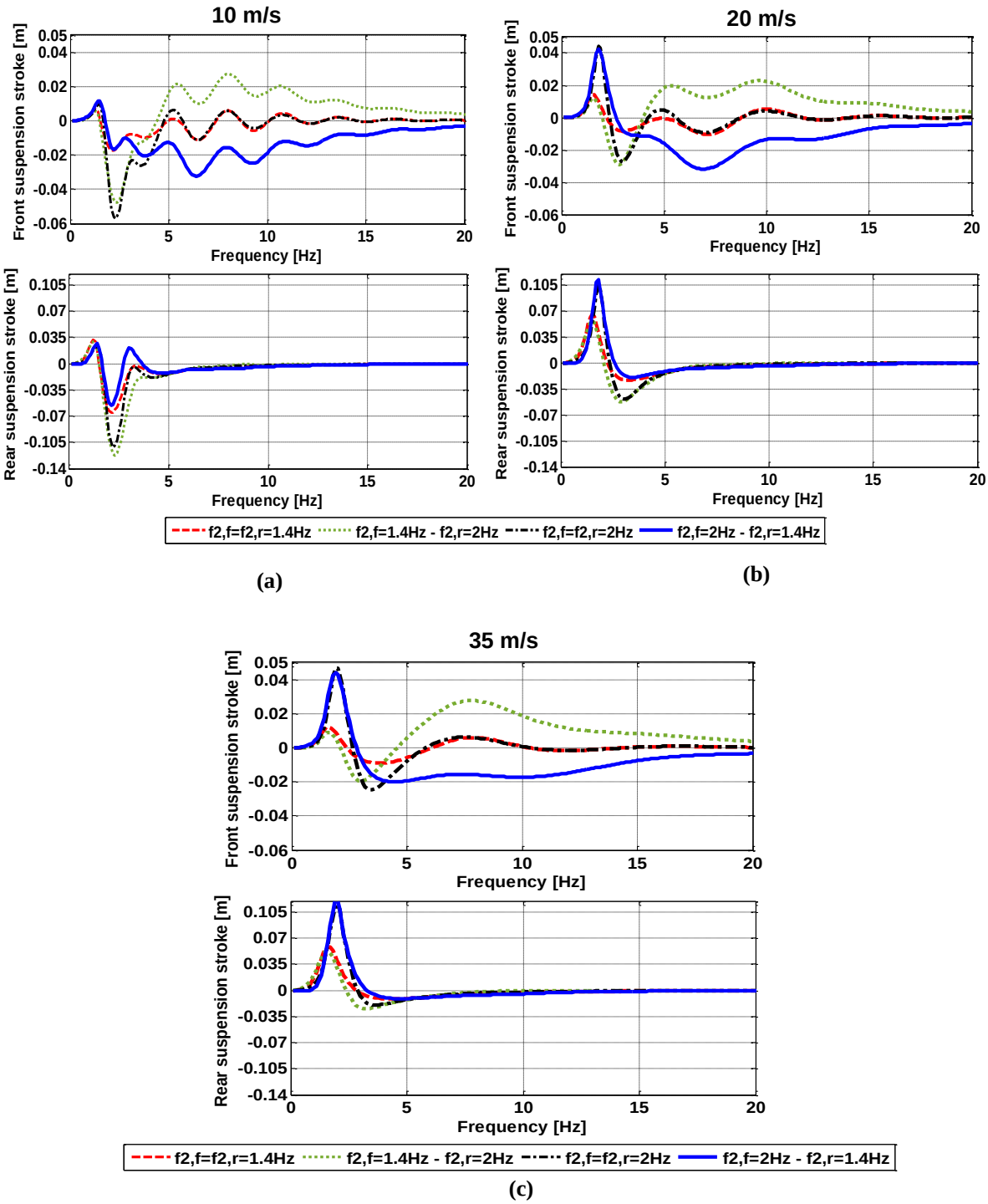

Figure 8. Front and rear suspension strokes

As for the suspension stroke amplitudes, the front suspension stroke movement achieves a maximum of 0.060m expansion and 0.045m compression movement at low frequencies, while the rear suspension achieved a stroke of 0.105 m for both compressing and expanding. These stroke values are quite normal for a passenger vehicle suspension, when considering that the suspension systems of passenger cars have an average stroke of 0.14m.

Also, all suspension stroke values are instantaneously obtained and the resulting oscillations are damped in a very short time especially in the rear axle. However, the front suspension stroke varies according to the front and rear spring stiffness. Accordingly, when the rear suspension is harder, the front suspension meets the road input with more closure, while the softer rear suspension meets the expanding. This is seen in Figure 8 where it is met with lower oscillations with increased vehicle speed.

4. CONCLUSIONS

The purpose of this paper is to reduce dynamic wheel loads and to determine the location of oscillation centers which reduce dynamic wheel loads. For this, the coupling is obtained by changing oscillation centers of pitch and bounce motions. In order to change the location of oscillation centres with different front and rear suspension stiffnesses, the half car model, which two quarter car models are combined by changing suspension stiffness and damping ratio and coupling the pitch motion to bounce motion, was used. In this way, the effects of changes in front suspension settings were reflected on those of rear suspension through different stiffnesses and damping ratios.

The frequency responses of the oscillations are obtained to investigate the effects of coupling on dynamic wheel load oscillations. The frequency responses show that if the oscillation center is changed depending on suspension stiffness without changing front and rear damping capacities, both of front and rear wheel load oscillations are not improved. Similarly, if the damping capacity of damper on the wheel connecting to stiff suspension becomes hard, either front or rear oscillation can be reduced at only vehicle body resonance area. The reason of this is that the dynamic load oscillations of wheel, to which CG and pitch center are close, are deteriorated without any change in damping capacity of damper.

On the other hand, as long as the damper connecting with soft suspension becomes hard, the changes in location of pitch and bounce centers can improve the dynamic wheel load oscillations at axle resonance regions. In here, it is considerable point that if the pitch and bounce centers are on same front wheel, both of front and rear oscillations can be reduced. Also, ride comfort and suspension stroke analysis were carried out to determine the suitability of the suspension stroke, which will provide ride comfort during the oscillation center change.

As a result, in this study, the most convenient oscillation center location to reduce dynamic wheel load oscillations has been determined without deteriorating ride comfort. This improvement has been obtained by varying available coupling with the changes in location of oscillation center. In further study, the results obtained in this study can be used with passive suspension with interconnedted springs or dampers and air suspension. Also, the dynamic wheel load oscillations are greatly reduced at resonance frequency of axle by changing damping level of front and rear dampers via active shock absorbers.

DECLARATION OF ETHICAL STANDARDS

The author(s) of this article declare that the materials and methods used in this study do not require ethical committee permission and/or legal-special permission.

AUTHORS' CONTRIBUTIONS

Hakan KÖYLÜ : created the mathematical model for vehicle pitch and bounce motions, conducted analyzes with different suspension parameters and evaluated the analysis results

CONFLICT OF INTEREST

There is no conflict of interest in this study.

REFERENCES

[1] Cao, D., Song, X. and Ahmadian, M., "Editors' perspectives: road vehicle suspension design, dynamics, and control", ***Vehicle System Dynamics***, 49(1): 3 -28, (2011).

[2] Sharp, R.S., "Road Vehicle Suspension System Design-A Review", ***Vehicle System Dynamics***, 16: 167- 192, (1987).

[3] Güney, A., "***The vibration and noise in vehicles: lecture notes***", Istanbul Technical University, (2002).

[4] Sun, T., Zhang. Y., Barak. P., "4-DOF vehicle ride model", ***SAE Paper***, 2002-01-1580, (2002).

[5] Milliken, F.W. and Milliken, D.L.,"***Chasis Design Principle and Analysis***", Society of Automotive Engineers, USA, (2002).

[6] Crolla, D.A. and King, R.P., "Olley's flat ride revisited", ***Vehicle System Dynamics,*** Supp. 33: 762–774, (1999).

[7] Olley, M., "Independent wheel suspension—its whys and wherefores", ***SAE Transactions***, 29: 73–81, (1934).

[8] Wong, J.Y.,"***Theory of ground vehicles***", second edition, John Wiley & Sons, (1993).

[9] Sharp R.S. and Pilbeam, C., "Achievability and value of passive suspension designs for minimum pitch response", ***In: ImechE International Conference–Vehicle Ride and Handling***, Birmingham, 15–17, (1993).

[10] Smith, W.A and Nong, Z., "Recent developments in passive interconnected vehicle suspension", ***Front. Mech. Eng***. 5(1): 1–18. (2010).

[11] Genta, G., "***Motor Vehicle Dynamics***", World Scientific, USA, (1992).

[12] Gillespie, T.D., "***Fundamentals of Vehicle Dynamics****"*, Society of Automotive Engineers, USA, (1992).

[13] Mitschke, M., "***Dynamik Der Kraftfahrzeuge Band B: Schwingungen***", Springer Verlag, Berlin, Germany, (1997).

[14] Xu, G., "***Investigation to the Ride and Handling of Vehicle with Interconnected Suspensions***", Doctoral Thesis, University of Technology, Sydney, (2016).

[15] Nagai, M and Hasegawa, T.. "Vibration isolation analysis and semi-active control of vehicles with connected front and rear suspension dampers", ***JSAE Review***, 18: 45-50, (1997).

[16] Dixon, J.C., "***The Shock Absorber Handbook",*** Second Edition, John Wiley & Sons, England, (2007).

[17] Cao, D., Rakheja, S., Su, C.Y., "Heavy vehicle pitch dynamics and suspension tuning. Part I: unconnected suspension", ***Vehicle System Dynamics***, 46(10): 931 – 953, (2008).

[18] Sharp, R.S.**, "**Wheelbase filtering and automobile suspension tuning for minimizing motions in pitch", ***Proceedings of the institution of mechanical engineers, Part D: J. Automobile Engineering***, 216: 933-946, (2002).

[19] Cao, D., Khajepour, A., Song, X., "Wheelbase Filtering and Characterization of Road Profiles for Vehicle Dynamics", ***12th AMSE International Conference on Advanced Vehicle and Tire Technologies***, Montreal, Canada, (2010).

[20] Xu, G., Zhang, N., Roser, H.M., "Roll and pitch independently tuned interconnected suspension: modelling and dynamic analysis", ***Vehicle System Dynamics***, 53:12, 1830-1849, (2015).

[21] Zhang, J., Deng, Y., Zhang, N., Zhang, B., Qi, Hengmin, Zheng, M., Vibration Performance Analysis of a Mining Vehicle with Bounce and Pitch Tuned Hydraulically Interconnected Suspension", ***Chin. J. Mech. Eng***, 32:5, (2019).

[22] Sharp, R.S., "Influences of suspension kinematics on pitching dynamics of cars in longitudinal maneuvering", ***Vehicle System Dynamics***, Suppl. 33: 23–36, (1999).

[23] Odhams, A.M.C. and Cebon, D., "An analysis of ride coupling in automobile suspensions", ***Proceedings of the institution of mechanical engineers, Part D: J. Automobile Engineering***, 220: 1041–1061, (2006).

APPENDIX A

1. Jacobian matrix (J_{Ek}) for kinetics energy

The first derivatives of kinetics energy with respect to vertical velocities for Jacobian matrix is as follows:

$$\frac{\partial Ek}{\partial \dot{z}_{2,f}} = Ek_{2,f},\ \frac{\partial Ek}{\partial \dot{z}_{2,r}} = Ek_{2,r},\ \frac{\partial Ek}{\partial \dot{z}_{1,f}} = Ek_{1,f},\ \frac{\partial Ek}{\partial \dot{z}_{1,r}} = Ek_{1,r}$$

If **z** is a function of and E_k is a function of ($Ek_{2,f}$, $Ek_{2,r}$, $Ek_{1,f}$, $Ek_{1,r}$), then the following matrix ,which shows four functions with four independent variables $(\dot{z}_{2,f}, \dot{z}_{2,r}, \dot{z}_{1,f}, \dot{z}_{1,r})$ is obtained. Note that $\mathbf{E_k}$ and **z** are vectors.

$$\mathbf{E_k}(\mathbf{z}) = \begin{bmatrix} Ek_{2,f}(\dot{z}_{2,f}, \dot{z}_{2,r}, \dot{z}_{1,f}, \dot{z}_{1,r}) \\ Ek_{2,r}(\dot{z}_{2,f}, \dot{z}_{2,r}, \dot{z}_{1,f}, \dot{z}_{1,r}) \\ Ek_{1,f}(\dot{z}_{2,f}, \dot{z}_{2,r}, \dot{z}_{1,f}, \dot{z}_{1,r}) \\ Ek_{1,r}(\dot{z}_{2,f}, \dot{z}_{2,r}, \dot{z}_{1,f}, \dot{z}_{1,r}) \end{bmatrix}$$

Hence, Jacobian matrix, which is known as the matrix of patial derivatives and is shown by $D\mathbf{E_k}(\mathbf{z})$ notation, is of the following form.

$$D\mathbf{E_k}(\mathbf{z}) = J_{Ek} = \begin{bmatrix} \frac{\partial Ek_{2,f}}{\partial \dot{z}_{2,f}} & \frac{\partial Ek_{2,f}}{\partial \dot{z}_{2,r}} & \frac{\partial Ek_{2,f}}{\partial \dot{z}_{1,f}} & \frac{\partial Ek_{2,f}}{\partial \dot{z}_{1,r}} \\ \frac{\partial Ek_{2,r}}{\partial \dot{z}_{2,f}} & \frac{\partial Ek_{2,r}}{\partial \dot{z}_{2,r}} & \frac{\partial Ek_{2,r}}{\partial \dot{z}_{1,f}} & \frac{\partial Ek_{2,r}}{\partial \dot{z}_{1,r}} \\ \frac{\partial Ek_{1,f}}{\partial \dot{z}_{2,f}} & \frac{\partial Ek_{1,f}}{\partial \dot{z}_{2,r}} & \frac{\partial Ek_{1,f}}{\partial \dot{z}_{1,f}} & \frac{\partial Ek_{1,f}}{\partial \dot{z}_{1,r}} \\ \frac{\partial Ek_{1,r}}{\partial \dot{z}_{2,f}} & \frac{\partial Ek_{1,r}}{\partial \dot{z}_{2,r}} & \frac{\partial Ek_{1,r}}{\partial \dot{z}_{1,f}} & \frac{\partial Ek_{1,r}}{\partial \dot{z}_{1,r}} \end{bmatrix}$$

2. Jacobian matrix (J_{Ep}) for stored potential enegy in suspension spring

The first derivatives of potential energy with respect to vertical displacements $z_{2,f}$, $z_{2,r}$, $z_{1,f}$, $z_{1,r}$ for Jacobian matrix is as follows:

$$\frac{\partial Ep}{\partial z_{2,f}} = Ep_{2,f},\ \frac{\partial Ep}{\partial z_{2,r}} = Ep_{2,r},\ \frac{\partial Ep}{\partial z_{1,f}} = Ep_{1,f},\ \frac{\partial Ep}{\partial z_{1,r}} = Ep_{1,r}$$

If **z** is a function of ($z_{2,f}$, $z_{2,r}$, $z_{1,f}$, $z_{1,r}$) and $\mathbf{E_p}$ is a function of ($Ep_{2,f}$, $Ep_{2,r}$, $Ep_{1,f}$, $Ep_{1,r}$), then the following matrix, which shows four functions with four independent variables ($z_{2,f}$, $z_{2,r}$, $z_{1,f}$, $z_{1,r}$), is obtained. Note that $\mathbf{E_p}$ and **z** are vectors.

$$\mathbf{E_p}(\mathbf{z}) = \begin{bmatrix} Ep_{2,f}(z_{2,f}, z_{2,r}, z_{1,f}, z_{1,r}) \\ Ep_{2,r}(z_{2,f}, z_{2,r}, z_{1,f}, z_{1,r}) \\ Ep_{1,f}(z_{2,f}, z_{2,r}, z_{1,f}, z_{1,r}) \\ Ep_{1,r}(z_{2,f}, z_{2,r}, z_{1,f}, z_{1,r}) \end{bmatrix}$$

Hence, Jacobian matrix for stored potential enegy in suspension spring is as follows:

$$D\mathbf{E_p}(\mathbf{z}) = J_{Ep} = \begin{bmatrix} \frac{\partial Ep_{2,f}}{\partial z_{2,f}} & \frac{\partial Ep_{2,f}}{\partial z_{2,r}} & \frac{\partial Ep_{2,f}}{\partial z_{1,f}} & \frac{\partial Ep_{2,f}}{\partial z_{1,r}} \\ \frac{\partial Ep_{2,r}}{\partial z_{2,f}} & \frac{\partial Ep_{2,r}}{\partial z_{2,r}} & \frac{\partial Ep_{2,r}}{\partial z_{1,f}} & \frac{\partial Ep_{2,r}}{\partial z_{1,r}} \\ \frac{\partial Ep_{1,f}}{\partial z_{2,f}} & \frac{\partial Ep_{1,f}}{\partial z_{2,r}} & \frac{\partial Ep_{1,f}}{\partial z_{1,f}} & \frac{\partial Ep_{1,r}}{\partial z_{1,r}} \\ \frac{\partial Ep_{1,r}}{\partial z_{2,f}} & \frac{\partial Ep_{1,r}}{\partial z_{2,r}} & \frac{\partial Ep_{1,r}}{\partial z_{1,f}} & \frac{\partial Ep_{1,r}}{\partial z_{1,r}} \end{bmatrix}$$

3. Jacobian matrix for dissipated enegy in shock absorber

The first derivative of kinetics energy with respect to vertical velocities for Jacobian matrix is as follows:

$$\frac{\partial Ed}{\partial \dot{z}_{2,f}} = Ed_{2,f},\ \frac{\partial Ed}{\partial \dot{z}_{2,r}} = Ed_{2,r},\ \frac{\partial Ed}{\partial \dot{z}_{1,f}} = Ed_{1,f},\ \frac{\partial Ed}{\partial \dot{z}_{1,r}} = Ed_{1,r}$$

If **z** is a function of $z_{2,f}$, $z_{2,r}$, $z_{1,f}$, $z_{1,r}$ and $\mathbf{E_d}$ is a function of ($Ed_{2,f}$, $Ed_{2,r}$, $Ed_{1,f}$, $Ed_{1,r}$), then the following matrix ,which shows four functions with four independent variables $(\dot{z}_{2,f}, \dot{z}_{2,r}, \dot{z}_{1,f}, \dot{z}_{1,r})$ is obtained. Note that $\mathbf{E_d}$ and **z** are vectors.

$$\mathbf{E_d}(\mathbf{z}) = \begin{bmatrix} Ed_{2,f}(\dot{z}_{2,f}, \dot{z}_{2,r}, \dot{z}_{1,f}, \dot{z}_{1,r}) \\ Ed_{2,r}(\dot{z}_{2,f}, \dot{z}_{2,r}, \dot{z}_{1,f}, \dot{z}_{1,r}) \\ Ed_{1,f}(\dot{z}_{2,f}, \dot{z}_{2,r}, \dot{z}_{1,f}, \dot{z}_{1,r}) \\ Ed_{1,r}(\dot{z}_{2,f}, \dot{z}_{2,r}, \dot{z}_{1,f}, \dot{z}_{1,r}) \end{bmatrix}$$

Hence, Jacobian matrix for dissipated enegy in shock absorber is of the following form.

$$D\mathbf{E_d}(\mathbf{z}) = J_{Ed} = \begin{bmatrix} \frac{\partial Ed_{2,f}}{\partial \dot{z}_{2,f}} & \frac{\partial Ed_{2,f}}{\partial \dot{z}_{2,r}} & \frac{\partial Ed_{2,f}}{\partial \dot{z}_{1,f}} & \frac{\partial Ed_{2,f}}{\partial \dot{z}_{1,r}} \\ \frac{\partial Ed_{2,r}}{\partial \dot{z}_{2,f}} & \frac{\partial Ed_{2,r}}{\partial \dot{z}_{2,r}} & \frac{\partial Ed_{2,r}}{\partial \dot{z}_{1,f}} & \frac{\partial Ed_{2,r}}{\partial \dot{z}_{1,r}} \\ \frac{\partial Ed_{1,f}}{\partial \dot{z}_{2,f}} & \frac{\partial Ed_{1,f}}{\partial \dot{z}_{2,r}} & \frac{\partial Ed_{1,f}}{\partial \dot{z}_{1,f}} & \frac{\partial Ed_{1,f}}{\partial \dot{z}_{1,r}} \\ \frac{\partial Ed_{1,r}}{\partial \dot{z}_{2,f}} & \frac{\partial Ed_{1,r}}{\partial \dot{z}_{2,r}} & \frac{\partial Ed_{1,r}}{\partial \dot{z}_{1,f}} & \frac{\partial Ed_{1,r}}{\partial \dot{z}_{1,r}} \end{bmatrix}$$